Developmental Biology 410 (2016) 86–97

Contents lists available at ScienceDirect

Developmental Biology

journal homepage: www.elsevier.com/locate/developmentalbiology

Defective myogenesis in the absence of the muscle-specific lysine methyltransferase SMYD1

Harika Nagandla [a], Suhujey Lopez [a], Wei Yu [a], Tara L. Rasmussen [b,c], Haley O. Tucker [c], Robert J. Schwartz [a,d], M. David Stewart [a,*]

[a] Department of Biology and Biochemistry, University of Houston, Houston, TX, USA
[b] Lillehei Heart Institute, University of Minnesota, Minneapolis, MN, USA
[c] Molecular Biosciences and Institute for Cellular and Molecular Biology, University of Texas, Austin, TX, USA
[d] Stem Cell Engineering Department, Texas Heart Institute at St. Luke's Episcopal Hospital, Houston, TX, USA

ARTICLE INFO

Article history:
Received 9 July 2015
Received in revised form
7 December 2015
Accepted 7 December 2015
Available online 11 December 2015

Keywords:
Myogenesis
Development
Muscle
SMYD1
Methylation

ABSTRACT

The SMYD (SET and MYND domain) family of lysine methyltransferases harbor a unique structure in which the methyltransferase (SET) domain is intervened by a zinc finger protein–protein interaction MYND domain. SMYD proteins methylate both histone and non-histone substrates and participate in diverse biological processes including transcriptional regulation, DNA repair, proliferation and apoptosis. *Smyd1* is unique among the five family members in that it is specifically expressed in striated muscles. Smyd1 is critical for development of the right ventricle in mice. In zebrafish, Smyd1 is necessary for sarcomerogenesis in fast-twitch muscles. Smyd1 is expressed in the skeletal muscle lineage throughout myogenesis and in mature myofibers, shuttling from nucleus to cytosol during myoblast differentiation. Because of this expression pattern, we hypothesized that Smyd1 plays multiple roles at different stages of myogenesis. To determine the role of Smyd1 in mammalian myogenesis, we conditionally eliminated *Smyd1* from the skeletal muscle lineage at the myoblast stage using $Myf5^{cre}$. Deletion of *Smyd1* impaired myoblast differentiation, resulted in fewer myofibers and decreased expression of muscle-specific genes. Muscular defects were temporally restricted to the second wave of myogenesis. Thus, in addition to the previously described functions for Smyd1 in heart development and skeletal muscle sarcomerogenesis, these results point to a novel role for Smyd1 in myoblast differentiation.

1. Introduction

Congenital myopathies and muscular dystrophies arise from mutations within genes responsible for diverse aspects of myogenesis and myofiber homeostasis. Thus, understanding the molecular genetics of muscle development is paramount to developing the basic science foundation required to develop cures for these diseases. Mammalian skeletal myogenesis consists of two distinct phases producing primary and secondary myofibers, respectively. In mice, the primary/embryonic wave takes place from embryonic day (E) 10.5 to E12.5 and the secondary/fetal wave occurs from E14.5 to E17.5 (Biressi et al., 2007b). Primary muscle fibers first appear on E11.5, when a small fraction of embryonic myoblasts fuse. Secondary fibers are formed through fusion of fetal myoblasts with each other or with primary fibers. From E15.5 onwards, smaller secondary fibers can be found adjacent to bigger primary fibers. Fetal myogenesis is also characterized by inception of innervation (Rossi and Messina, 2014). The myogenic cells that give rise to these two waves have been well documented to have distinct characteristics in terms of the genes they express, the features of the myotubes they produce *in vitro* and their response to inhibitors of myogenesis and growth factors (Biressi et al., 2007b). In general, primary fibers are similar to adult slow-twitch muscle fibers while secondary fibers exhibit characteristics of adult fast-twitch muscle fibers (Biressi et al., 2007a).

The SMYD (SET and MYND domain) family of lysine methyltransferases is defined by a unique structure in which the methyltransferase (SET) domain is intervened by a zinc finger protein–protein interaction MYND domain (Spellmon et al., 2015). SMYD proteins are implicated in a vast number of biological processes including transcriptional activation/repression (Huang et al., 2006; Xu et al., 2015), DNA repair (Piao et al., 2014), cell cycle (Cho et al., 2012; Saddic et al., 2010), tumorigenesis (Luo et al., 2014; Mazur et al., 2014) and apoptosis (Sajjad et al., 2014). *Smyd1*

* Correspondence to: Department of Biology & Biochemistry, University of Houston, 3455 Cullen Blvd, Houston, TX 77204-5001 USA.
E-mail address: dstewart@uh.edu (M.D. Stewart).

http://dx.doi.org/10.1016/j.ydbio.2015.12.005
0012-1606/

is unique among the five family members in that its expression (*a* and *b* isoforms) is restricted to striated muscles; a third *c* isoform is expressed in $CD8^+$ T cells (Gottlieb et al., 2002; Hwang and Gottlieb, 1997). Smyd1 harbors both transcriptional activation and repression activities and methylates both histone and non-histone substrates (Rasmussen et al., 2015; Tan et al., 2006). Smyd1 methylates histone H3 at lysine 4, a modification associated with active transcription (Tan et al., 2006), but Smyd1 represses transcription when tethered to DNA by recruitment of HDAC1, -2 or -3 to its MYND domain (Sims et al., 2002). The MYND domain is also the site of interaction with the muscle-specific transcription factor skNAC (Sims et al., 2002), the only transcription factor known to associate with Smyd1. Smyd1 methylates the cardiac endoplasmic reticulum stress sensor TRB3, which in turn, serves as a corepressor for Smyd1 (Rasmussen et al., 2015). Expression of *Smyd1* in muscle is regulated by a number of factors such as MEF2C, SRF, Myogenin and HDGF (Li et al., 2009; Phan et al., 2005; Yang and Everett, 2009). Conventional knockout of *Smyd1* in mice results in embryonic lethality by E10.5 due to failure in right ventricular development (Gottlieb et al., 2002).

Due to embryonic lethality prior to myogenesis in mice (Gottlieb et al., 2002), most knowledge of Smyd1's function in skeletal muscle comes from studies in zebrafish (Du et al., 2006; Gao et al., 2014; Li et al., 2011, 2013; Tan et al., 2006) where it is critical for sarcomerogenesis in fast-twitch muscles (Just et al., 2011). Smyd1 co-localizes with nascent myosin during sarcomerogenesis and then to the M-line of mature sarcomeres. Antisense morpholino-based knock-down of both *Smyd1* isoforms in zebrafish embryos led to severe impairment of myofibrillogenesis in both skeletal and cardiac muscle. Myosin chaperones *Hsp90α1* and *UNC45b* were up regulated (Just et al., 2011; Li et al., 2013), suggesting that thick filament assembly is impaired in the absence of Smyd1. Smyd1's physical interaction with myosin is crucial for proper myofibrillar arrangement in zebrafish skeletal muscle (Just et al., 2011). These data indicate that Smyd1 is an important facilitator of myofibrillogenesis.

Based on gene expression and protein localization, we hypothesized that *Smyd1* also plays a role in early myogenesis. In *Xenopus laevis*, chick and zebrafish embryos, *Smyd1* is expressed in the somites at the onset of myogenesis (Du et al., 2006; Gottlieb et al., 2002; Just et al., 2011; Kawamura et al., 2008). Expression persists throughout myogenesis and in mature myofibers. The subcellular localization of Smyd1 during myogenesis has been studied *in vitro* using mouse C2C12 myoblasts (Sims et al., 2002). In C2C12 cells, *Smyd1* expression increases tremendously during the transition from myoblast to myotubes (Berkholz et al., 2014; Li et al., 2009; Sims et al., 2002). Smyd1 localizes to the nucleus and cytoplasm of myoblasts; however, after fusion, Smyd1 mostly resides in the cytoplasm of myotubes (Berkholz et al., 2014; Sims et al., 2002). This nuclear to cytoplasmic translocation of Smyd1 during myoblast differentiation is regulated by sumoylation—as inhibition of sumoylation resulted in nuclear accumulation of Smyd1 and reduced terminal differentiation (Berkholz et al., 2014). These data suggest a role for Smyd1 in the formation of myotubes during embryogenesis.

The purpose of this study was to elucidate Smyd1's role during skeletal myogenesis in mice. To this end, we conditionally eliminated *Smyd1* from early muscle precursor cells using $Myf5^{cre}$. Deletion of *Smyd1* in early myoblasts did not affect proliferation, but instead impaired differentiation, resulting in fewer muscle fibers and decreased expression of skeletal muscle-specific genes. Muscular defects were temporally restricted to the second myogenic wave. Thus, in addition to the previously described functions for Smyd1 in expansion of second heart field progenitor cells, maturation of cardiomyocytes, antagonizing cardiomyocyte stress responses and skeletal muscle sarcomerogenesis, these results point to a novel role for Smyd1 in myoblast differentiation.

2. Results

2.1. Smyd1 expression and subcellular localization during myogenesis.

A previous analysis of *Smyd1* spatial expression during embryogenesis showed *Smyd1* mRNA to be expressed very specifically in the heart and somites of chick embryos by Hamburger and Hamilton stage 20 (Gottlieb et al., 2002). Similar expression was reported for zebrafish embryos (Du et al., 2006; Just et al., 2011; Tan et al., 2006). However, in E10.5 mouse embryos, *Smyd1* mRNA was detected in the heart, but not the somites (Gottlieb et al., 2002). To reconcile this difference, we assayed the spatial expression of *Smyd1* mRNA in mouse embryos at E9.5 by *in situ* hybridization. In agreement with chick and zebrafish experiments, *Smyd1* mRNA was very specifically expressed in both somites and heart (Fig. 1A). These data confirm that *Smyd1* is a striated muscle-specific methyltransferase with initial onset of expression in the skeletal muscle linage occurring prior to the appearance of myofibers.

$Myf5^{cre}$ mice harbor an *IRES-cre* knock-in within the 5' UTR of the *Myf5* gene (Haldar et al., 2007); therefore, *cre* expression should be restricted to somitic myoblasts and absent from cardiac lineages. We confirmed this activity using the $Rosa26^{YFP}$ reporter. Cre-induced recombination of *loxP* sites occurred very specifically in the somites and not in the heart (the other site of *Smyd1* expression) (Fig. 1B). These data illustrate the utility of this genetic cross to delete *Smyd1* at the earliest stage of its expression in the skeletal muscle lineage without affecting heart development.

It was reported that the subcellular localization of Smyd1 changes during C2C12 myoblast differentiation (Berkholz et al., 2014; Sims et al., 2002); however, this has yet to be observed for endogenous Smyd1 during myogenesis *in vivo*. First, we confirmed previous reports showing export of Smyd1 from nucleus to cytosol during C2C12 differentiation. Smyd1 localized to both the nucleus and cytoplasm in undifferentiated C2C12 myoblasts (Fig. 1C). After 5 days in differentiation medium, Smyd1 localized primarily to the cytosol of myotubes (Fig. 1D). Relatively low levels of fluorescence were still detectable in the nucleus. Thus, while the majority of Smyd1 protein is cytoplasmic in myotubes, a small fraction remains in the nucleus with the potential to regulate transcription.

Next, we determined spatial and temporal expression of Smyd1 during myogenesis *in vivo*. Within the myotome at E11.5, Smyd1 and Pax7 did not co-localize (Fig. 1E–I), thus representing distinct cell populations. In contrast, Smyd1 co-localized with Myogenin (Myog) in many cells (Fig. 1J–N, white arrowheads in panel M). Individual cells could be observed expressing Myog, but little to no Smyd1 (Fig. 1M, yellow arrowheads). Cells expressing high Smyd1 with low Myog are likely newly formed primary fibers (Fig. 1M, purple arrowheads). Similar results were observed in skeletal muscle at E16.5 (Fig. 1O–S). At this stage, Smyd1 protein is abundant in the sarcoplasm of all fibers with relatively lower levels in myonuclei. Smyd1 colocalized with Myog in many newly forming secondary fibers (Fig. 1R, white arrowheads). A small number of cells expressed Myog, but little to no Smyd1 (Fig. 1R, yellow arrowheads). Collectively, these data indicate that Smyd1 is downstream of Pax7 and Myog, being expressed in $Myog^+$ myoblasts, but not $Pax7^+$ progenitor cells.

Previous reports showed that Smyd1 localizes to the M-line of muscle fibers in zebrafish (Just et al., 2011; Li et al., 2011). Indeed by E15.5 and in adult muscle, Smyd1 exhibited a characteristic sarcomeric localization pattern with alternating bands of α-actinin and Smyd1 (Fig. 1T, U). These results are consistent with the

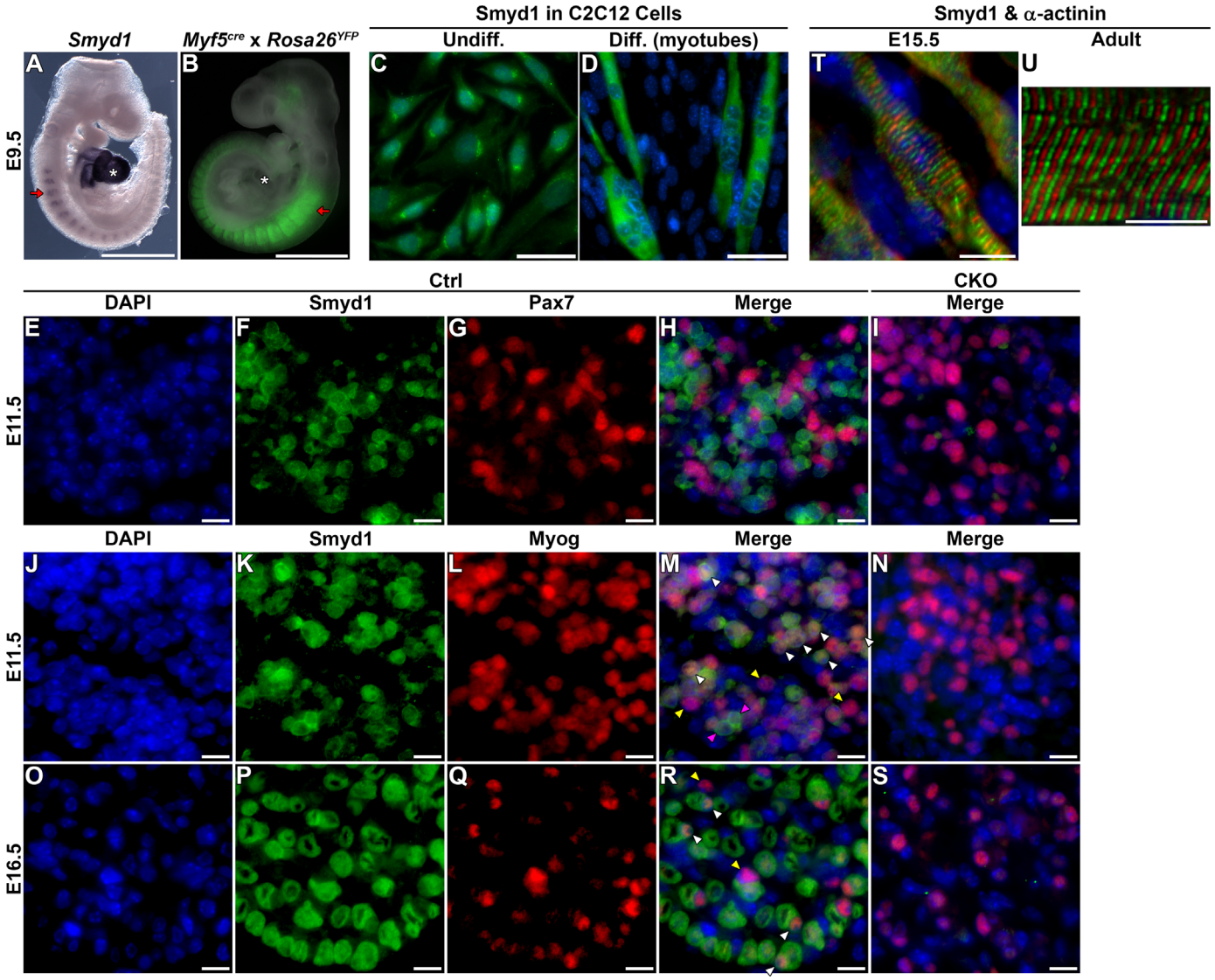

Fig. 1. *Smyd1* expression and subcellular localization during myogenesis. (A) Whole mount *in situ* hybridization for *Smyd1* mRNA at E9.5. *Smyd1* mRNA is specifically localized to the heart (white asterisk) and somites (red arrow). (B) Stereoimage overlay of YFP fluorescence (green) and brightfield. *Myf5*^{cre} is specifically active in the somites (red arrow), but not the heart (white asterisk). (C, D) Immunofluorescence for Smyd1 (green) in undifferentiated C2C12 myoblasts (C) or myotubes after five days in differentiation medium (D). (E–I) Immunofluorescence for Smyd1 (green) and Pax7 (red) in the myotome of control (E–H) or *Smyd1* CKO (I) embryos at E11.5. (J–N) Immunofluorescence for Smyd1 (green) and Myog (red) in the myotome of control (J-M) or *Smyd1* CKO (N) embryos at E11.5. (O–S) Immunofluorescence for Smyd1 (green) and Myog (red) in the EDL muscle of control (O–R) or *Smyd1* CKO (S) embryos at E16.5. (T, U) Immunofluorescence for Smyd1 (green) and α-actinin (red) in longitudinal skeletal muscle sections of wild-type embryos at E15.5 (T) and adult soleus muscle (U). Blue, nuclei (DAPI). (M, R) White arrowheads, co-localization of Smyd1 and Myog; yellow arrowheads, Myog^{+} Smyd1^{-} cells; purple arrowheads, young fibers with low Myog and high Smyd1. Scale bars are 1 mm (A, B), 50 μm (C, D) and 10 μm (E–U). Ctrl, control; CKO, conditional knockout.

conclusion that the majority of Smyd1 in differentiated fibers localizes to the M-line.

These data support a working model in which Smyd1 functions primarily as a nuclear transcriptional regulator during myoblast proliferation and differentiation. Later, as Smyd1 accumulates in myotube/myofiber sarcoplasm, it serves in sarcomere assembly and stability. Using *Myf5*^{cre}, we were able to deplete Smyd1 from myoblasts, at a time in which the protein is most likely to be affecting the myogenic transcriptional program.

2.2. *Smyd1 CKO embryos exhibit perinatal lethality*

Embryos from the cross *Myf5*$^{cre/+}$; *Smyd1*$^{+/-}$ x *Smyd1*$^{flox/flox}$; *Rosa26*$^{YFP/YFP}$ were recovered at various developmental stages (Table 1). The expected Mendelian percentage (25%) of CKO embryos were observed at all stages of gestation. However, embryos

Table 1
Smyd1 CKO embryos exhibit perinatal lethality.

Stage	Embryos Recovered	Expected CKOs	Observed CKOs
E9.5	20	5	7
E10.5	196	49	49
E11.5	9	2.25	2
E13.5	48	12	10
E14.5	8	2	1
E15.5	142	35.5	30
E16.5	45	11.25	17
E17.5	31	7.75	4 (motionless)
E18.5	16	4	4 (motionless)
*P0	53	13.25	6 (dead)

* $P=0.001$, Fisher's Exact Test; CKOs, conditional knockouts; E, embryonic day; P, postnatal day.

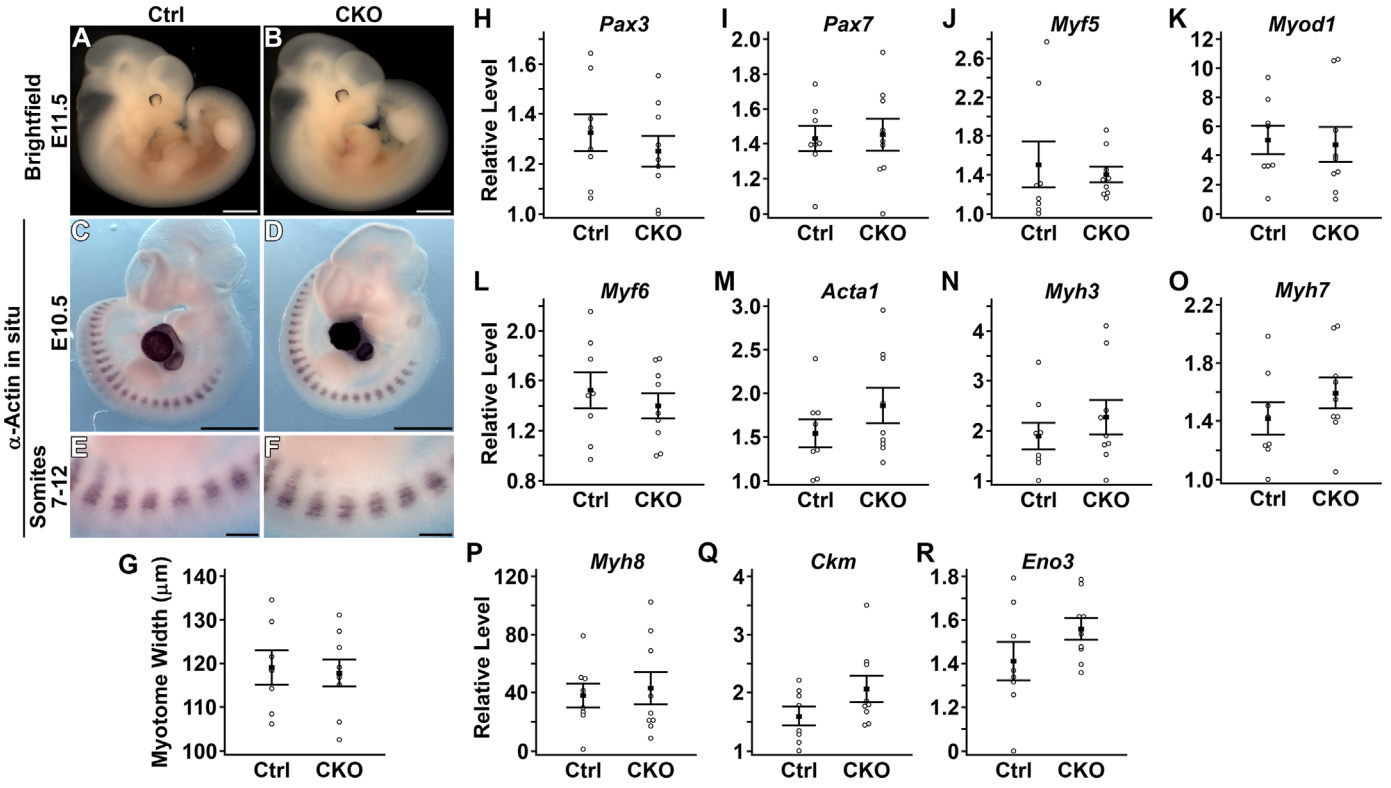

Fig. 2. *Smyd1* CKO embryos appear normal during the first wave of myogenesis. (A–B) Brightfield stereoimages of control (A) and *Smyd1* CKO (B) embryos at E11.5. (C–F) Whole mount *in situ* hybridization for α-*actin* mRNA in control (C, E) and *Smyd1* CKO (D, F) embryos at E10.5. (G) Measurement of myotome width (somites 7–12) using images such as illustrated in E and F. No difference was observed ($n \geq 7$ embryos/group). (H–R) Results of real-time PCR for myogenic transcription factors (H–L) and markers of differentiation (M–R) at E11.5. No differences in gene expression were observed ($n \geq 8$ embryos/group). Scale bars are 1 mm (A–D) and 200 μm (E, F). Student's *t* test. Error bars indicate SEM. Ctrl, control; CKO, conditional knockout.

recovered at E17.5 or E18.5 were motionless. Less than the expected number of *Smyd1* CKO pups were found on the day of birth (postnatal day 0) and those that were identified were dead. Thus, loss of *Smyd1* in the myogenic lineage produces perinatal lethality likely due to inability to breathe.

2.3. *Smyd1 CKO embryos appear normal during the first wave of myogenesis*

At E11.5, during the first wave of myogenesis, *Smyd1* CKO embryos were indistinguishable from control embryos (Fig. 2A, B). *In situ* hybridization for *α-actin* showed normal somitogenesis in *Smyd1* CKOs at E10.5 (Fig. 2C–F), with no difference in myotome width (somites 7–12) between controls and CKOs (Fig. 2G). We next tested whether loss of *Smyd1* affected muscle gene expression during the first wave of myogenesis. At E11.5, the midpoint of the first wave, mRNA expression of major myogenic transcription factors (*Pax3, Pax7, Myf5, Myod1* and *Myf6*) was equivalent between control and CKO embryos (Fig. 2H–L). At the same stage, expression of several genetic markers of differentiated myofibers (*Acta1* (α-actin), *Myh3* (embryonic MyHC), *Myh7* (slow MyHC), *Myh8* (Fetal MyHC), *Ckm* (creatine kinase) and *Eno3* (β-enolase)) was also equivalent (Fig. 2M–R). These data point to normal initiation of the skeletal myogenesis program in the absence of Smyd1.

2.4. *Smyd1 CKO embryos exhibit reduced muscle mass and subcutaneous edema during the second myogenic wave*

As expected, *Myf5*^{cre}-induced recombination was restricted to the skeletal muscle lineage, dorsal epidermis and brown adipose of control and *Smyd1* CKO embryos as determined by fluorescence from the *Rosa26*^{YFP} reporter (Fig. 3A–D). Loss of Smyd1 protein was confirmed by western blot using protein extracts from the body wall of E16.5 embryos (Fig. 3E). By E15.5, *Smyd1* CKO embryos were easily distinguished from control littermates by dorsal subcutaneous edema (Fig. 3F, G). Transverse tissue sections were prepared at the level of the forelimbs for H&E staining and immunofluorescence. In these sections, the dorsal subcutaneous edema manifested as a wide region of loose connective tissue between the skin and back muscles (Fig. 3H, I). This pathology may be similar to the "amorphous connective tissue" reported in *Myf5/MyoD* double knockout mice, which completely lack skeletal muscle (Rudnicki et al., 1993). Back muscles also appeared diminished in H&E sections (Fig. 3H, I). Relative myofiber abundance was determined by immunofluorescence for sarcomeric α-actinin. Far less α-actinin staining was observed in *Smyd1* CKO embryos (Fig. 3J, K), suggesting reduced muscle mass. Furthermore, in western blots, *Smyd1* CKO embryos exhibited 2.3-fold less total myosin heavy chain (MyHC) protein than controls (mean pixel intensity: Ctrl, 35.10 ± 6.56 u; CKO, 15.25 ± 3.29 u; $P=0.03$, Student's *t*-test) (Fig. 3E). These data indicate reduced muscle mass during the second wave of myogenesis in the absence of Smyd1.

2.5. *Fewer muscle fibers and reduced muscle gene expression during the second wave of myogenesis*

Myofiber abundance and organization was assayed by immunofluorescence using a pan-MyHC antibody. Longitudinal sections of the extensor digitorum longus (EDL) muscle showed disorganized arrangement of myofibers in *Smyd1* CKOs at E16.5 (Fig. 4A, B). Similarly stained transverse sections of EDL muscles revealed less densely packed myofibers and less anti-MyHC immunoreactivity in the *Smyd1* CKOs (Fig. 4C, D). Wide-field images

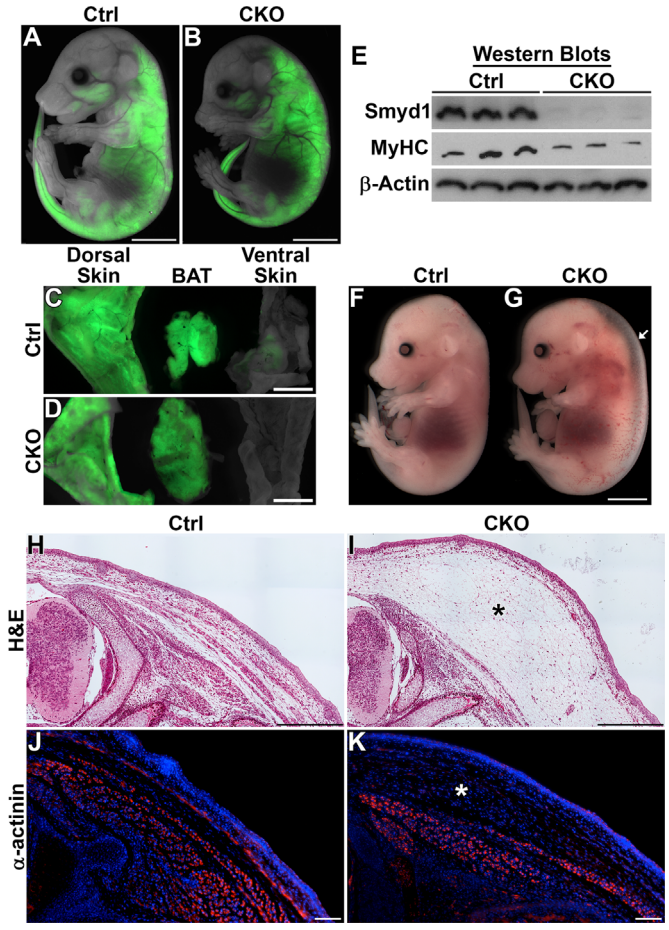

Fig. 3. *Smyd1* CKO embryos exhibit reduced muscle mass and subcutaneous edema. (A–D) Overlay of YFP (green) and brightfield stereofluorescence images at E15.5 showing *Myf5*^{cre} fate map. *Myf5* lineage cells are similarly distributed in skeletal muscles, tail and dorsal tissues of both control (A) and *Smyd1* CKO (B) embryos. *Myf5*$^{+}$ cells give rise to dorsal skin and brown adipose, but not ventral skin in both control (C) and *Smyd1* CKO (D) embryos. (E) Western blots using body wall extracts from E16.5 embryos. Smyd1 protein was undetectable in *Smyd1* CKO embryos. Total myosin heavy chain (MyHC) was reduced in *Smyd1* CKO embryos. Anti-β-actin was used as a loading control. (F, G) Brightfield stereoimages at E15.5. *Smyd1* CKO embryos exhibit subcutaneous edema (white arrow) across the length of the dorsal side. (H, I) H&E-stained transverse sections (dorsal quarter) at E15.5. A region of subcutaneous expanded loose connective tissue (black asterisk) is prominent in *Smyd1* CKO embryos. (J, K) Immunofluorescence for α-actinin (red) showing reduced abundance of myofibers in *Smyd1* CKO embryos at E15.5. Blue, nuclei (DAPI). White asterisk, subcutaneous edema. Scale bars are 2 mm (A–D, F, G), 500 μm (H, I) and 100 μm (J, K). BAT, brown adipose tissue; Ctrl, control; CKO, conditional knockout; MyHC, myosin heavy chain.

of tibialis anterior and EDL muscle sections can be found in Supplementary Fig. S1. The abundance of primary and secondary myofibers was quantified in transverse EDL sections such as those illustrated in Fig. 4C, D. Two sections each from nine CKO and ten control embryos were used for counting and normalized to cross-sectional area of the muscle. *Smyd1* CKOs exhibited significantly fewer primary and secondary fibers as compared to the controls (Fig. 4E, F). Secondary fiber development was impaired more than primary fiber development (22.3% reduction in primary fibers, 44.3% reduction in secondary fibers).

Next, we tested if the loss of myofibers was due to alterations in expression of myogenic transcription factors. Real-time PCR at E15.5 showed *Pax3*, which exhibits relatively higher expression in embryonic myoblasts and myotubes than in fetal myoblasts and myotubes (Biressi et al., 2007b), was elevated in the *Smyd1* CKO. *Pax7* and *Myod1* were unaffected; *Myf5* and *Myf6* were down-regulated (Fig. 4G–K). We next examined expression of genes associated with differentiated skeletal myocytes. mRNA levels of *Acta1* (α-actin), *Myh3* (embryonic MyHC), *Myh7* (slow MyHC), *Myh8* (fetal MyHC), *Ckm* (muscle creatine kinase) and *Eno3* (β-enolase) were all reduced in the *Smyd1* CKO at E15.5 (Fig. 4L–Q). These results indicate loss of Smyd1 impairs myofiber development during the second myogenic wave and support our observation of fewer muscle fibers in the *Smyd1* CKOs at E16.5.

We reasoned that reduced myofiber abundance could be the result of myofiber degeneration. To this end, we measured the width of the myosin ring surrounding nuclei of primary fibers and expression of atrophy-associated genes *Trim63/Murf1* and *Fbxo32/MAFbx/Atrogin1*. There was no difference in myofiber width (Fig. 4R) nor in expression of *Trim63* or *Fbxo32* (Fig. 4S, T). These data indicate that reduced myofiber abundance was not due to degeneration.

2.6. Loss of Smyd1 impairs myoblast differentiation

Next, we tested whether the reduction in myofibers was due to alterations in myoblast proliferation, differentiation or induced cell death. Transverse sections of E11.5 embryos at the depth of the forelimb bud were immuno-stained for Pax7. The myotomes of control and *Smyd1* CKO embryos displayed equivalent abundance of Pax7^{+} cells (Fig. 5A, B). The number of Pax7^{+} cells were counted and normalized with respect to total myotome nuclei. We found no difference in the number of Pax7-expressing myoblasts between control and *Smyd1* CKO embryos during the first wave of myogenesis (Fig. 5C). At E15.5, during the second wave of myogenesis, we performed a similar experiment using transverse sections of EDL muscles. Again, we observed no difference in the abundance of Pax7^{+} cells within EDL cross-sections (Fig. 5D, E). Quantification of the percentage of Pax7^{+} cells confirmed that conclusion (Fig. 5F). However, comparison of the total number of myofibers relative to the number of Pax7^{+} cells indicated that fewer myofibers arose from approximately the same number of Pax7^{+} myogenic progenitor cells in the *Smyd1* CKO (Fig. 5G). We next utilized expression of YFP from the *Rosa26*^{YFP} allele to compare the number of myofibers relative to non-myofiber *Myf5* lineage cells (myoblasts) in EDL cross-sections (Fig. 5H, I). We found a significant decrease in the number of myofibers per myoblast (Fig. 5J).

To determine if the observed reduction in *Smyd1* CKO myofiber density resulted from a myoblast proliferation defect, pregnant mice carrying E15.5 embryos were administered BrdU four hours prior to sacrifice. Proliferating myoblasts were identified by co-localization of BrdU and YFP in cross-sections of EDL muscle (Fig. 5K, L), and quantified as the percentage of total nuclei within the EDL (Fig. 5M). We observed no significant difference in proliferation rates between control and *Smyd1* CKO myoblasts. We then tested the most likely alternative explanation, apoptosis. TUNEL assays using E15.5 EDL cross-sections, however, identified very few (1-2/section) apoptotic cells in either control or *Smyd1* CKO embryos (Fig. 5N, O). In summary, we found reduced myofiber abundance in the presence of comparable numbers of Pax7^{+} myogenic precursor cells with no alterations in proliferation or apoptosis. These data implicated a downstream defect in myoblast differentiation. To test for a differentiation defect, we assayed the abundance of Myog^{+} cells (Fig. 5P, Q) and found a significant increase in the percentage of Myog^{+} cells within the EDL muscle of *Smyd1* CKO embryos (Fig. 5R). These data indicate that Smyd1 affects late stage myoblast differentiation.

2.7. Smyd1 knockdown in C2C12 myoblasts impairs fusion and blocks myotube hypertrophy

We employed the C2C12 mouse myoblast cell line to determine

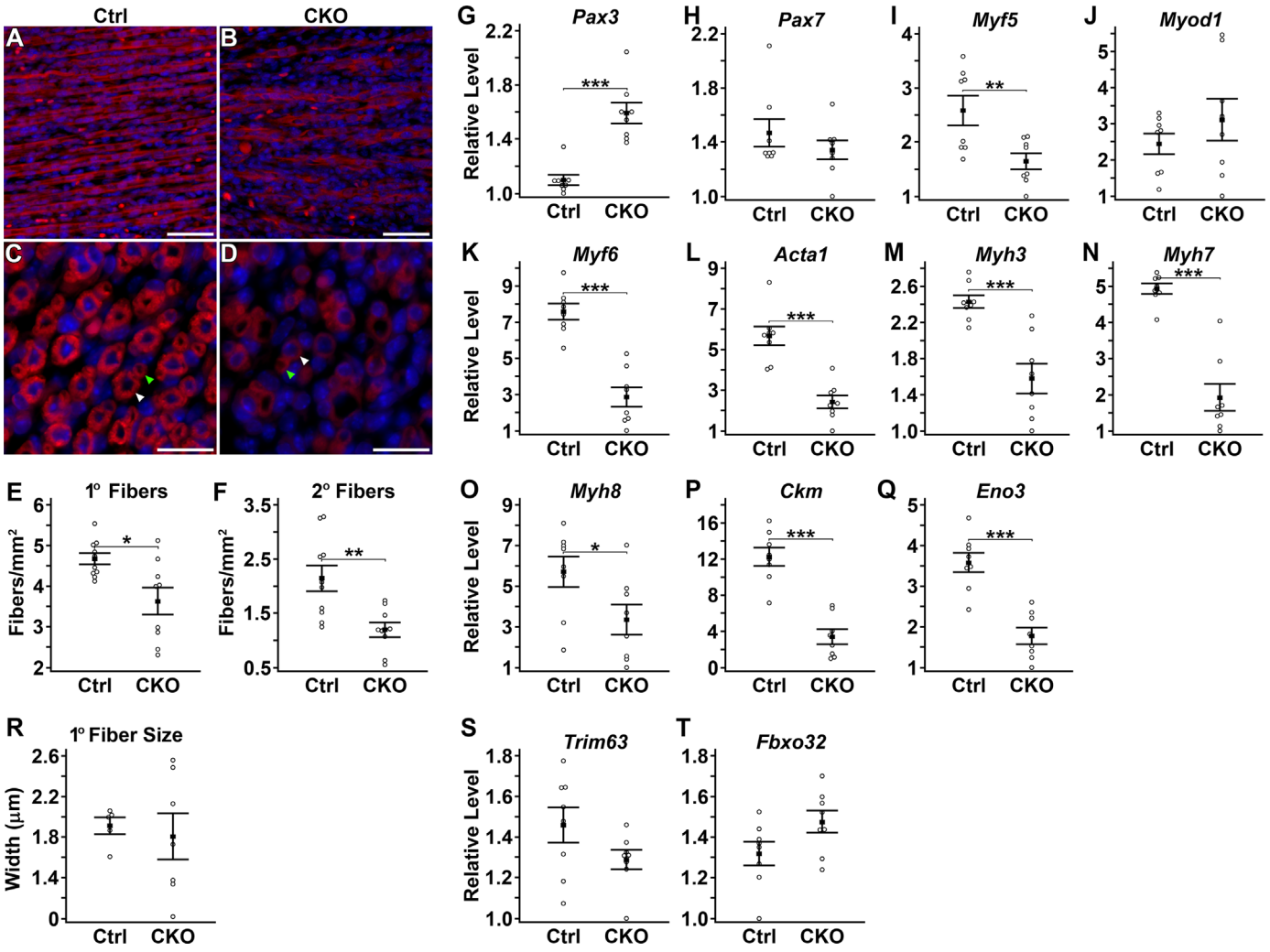

Fig. 4. Fewer muscle fibers and reduced muscle gene expression during second wave myogenesis. (A–D) Immunofluorescence for myosin heavy chain (red) in longitudinal (A, B) and transverse (C, D) sections of the EDL muscle at E16.5. Blue, nuclei (DAPI). White arrowhead, primary myofiber; green arrowhead, secondary myofiber. (E, F) Quantification of the number of primary (E) and secondary (F) myofibers in the EDL. *Smyd1* CKO EDL exhibited less primary and secondary fibers than controls ($n \geq 9$ embryos/group). (G–K) Expression of myogenic transcription factor genes in the body wall at E16.5 by real-time PCR ($n=8$ embryos/group). (L–Q) Real-time PCR assays for genes expressed in differentiated myofibers ($n=8$ embryos/group). (R) Thickness of myosin ring surrounding nuclei of primary fibers. No difference was observed ($n \geq 5$ embryos/group). (S, T) Real-time PCR assays for atrophy genes in the body wall at E16.5. No difference was observed ($n=8$ embryos/group). $^{*}P < 0.05$, $^{**}P < 0.01$, $^{***}P < 0.001$, Student's *t* test. Error bars indicate SEM. Scale bars are 50 μm. Ctrl, control; CKO, conditional knockout.

if *Smyd1* knockdown affects myoblast fusion or myotube growth. Previous studies reported that expression of *Smyd1* increases during myoblast differentiation (Li et al., 2009; Sims et al., 2002). First, we confirmed these reports by comparing Smyd1 protein levels in undifferentiated myoblasts vs. differentiated myotubes. Smyd1 protein was below the detectable threshold in undifferentiated myoblasts, but steadily increased after 1–5 days in differentiation medium (Fig. 6A). To reduce Smyd1 levels, C2C12 myoblasts were infected with lentivirus expressing shRNA against *Smyd1* or a non-specific control shRNA. After five days in differentiation medium, Smyd1 protein levels were reduced in two independently derived C2C12 clones that received *Smyd1* shRNA (1.5-fold and 3.1-fold, respectively). The clone that received the control lentivirus expressed Smyd1 at a similar level to that of the parental cell line (Fig. 6B). These clones were allowed to undergo differentiation for five days and then immuno-stained with a pan-MyHC antibody. *Smyd1* knockdown resulted in thin, hypotrophic myotubes (Fig. 6C, D). Myotube hypertrophy, as quantified by measuring myotube width at widest point on the myotube ($n=35$–60 myotubes/group × three technical replicates), was significantly decreased in cells that received *sh*RNA against *Smyd1* (Fig. 6F). As revealed by the distribution of myotubes plotted according to their width (Fig. 6G), *Smyd1* knockdown cell lines showed an increased number of small diameter myotubes. Next, a myoblast fusion index was calculated by dividing the number of nuclei incorporated into myotubes by the total nuclei in each field of view. *Smyd1* knockdown resulted in significantly fewer nuclei integrated into myotubes (Fig. 6E). These data indicate that Smyd1 regulates both myoblast fusion and myotube hypertrophy and support our *in vivo* observation of impaired myoblast differentiation in the *Smyd1* CKO.

3. Discussion

3.1. Spatial and temporal expression of Smyd1 during myogenesis

Previous reports of Smyd1's subcellular localization during myoblast differentiation have been limited to endogenous Smyd1 in C2C12 cells and transgenic expression of Myc-tagged Smyd1 in zebrafish. In C2C12 cells, Smyd1 shuttles from the nucleus to the cytoplasm during myoblast differentiation (Berkholz et al., 2014;

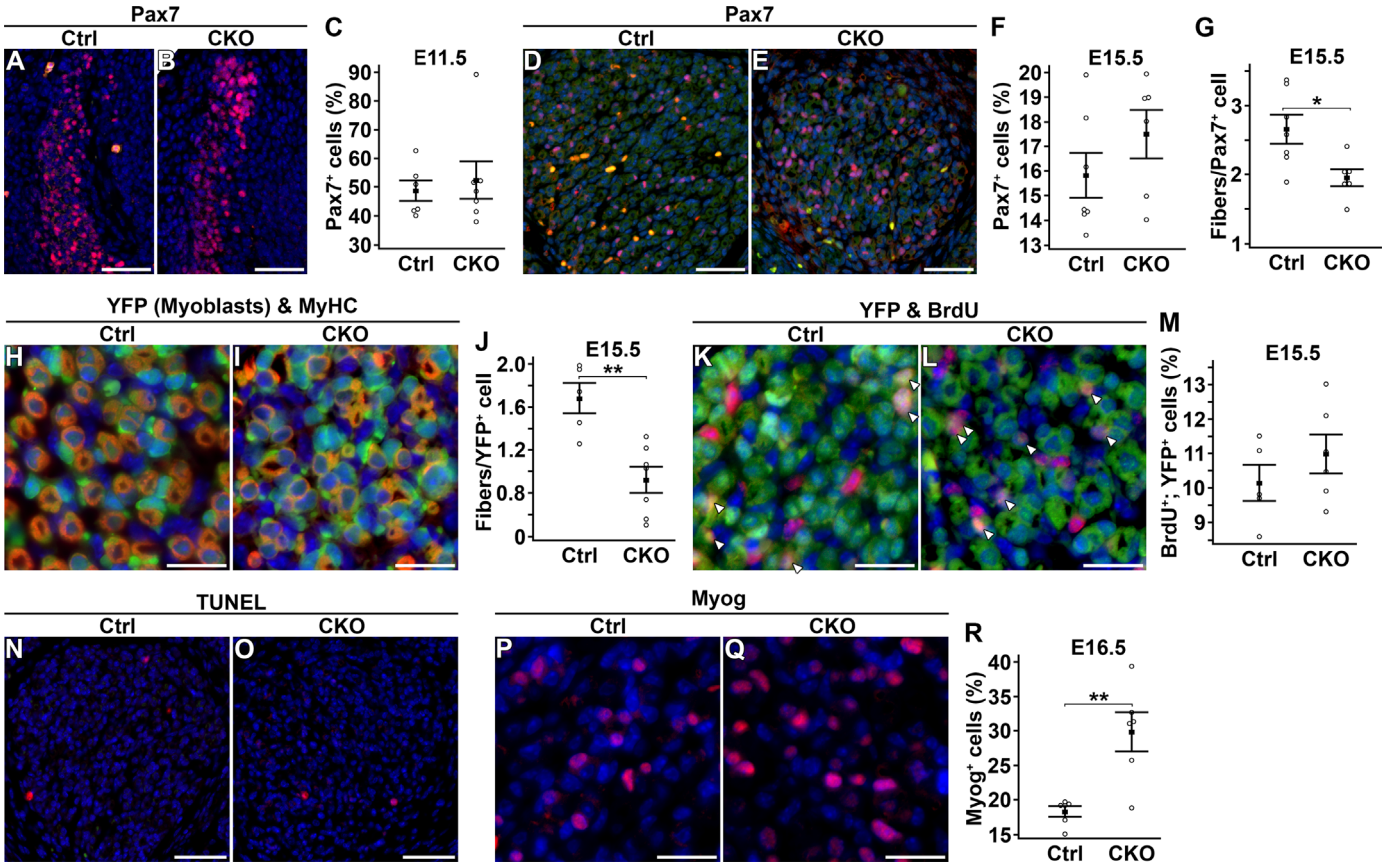

Fig. 5. Loss of *Smyd1* impairs myoblast differentiation. (A–C) Comparison of the number of Pax7$^+$ cells in the myotome at E11.5. (A, B) Representative images of Pax7 immunofluorescence (red). No difference was observed in the percentage of Pax7$^+$ cells in the myotome ($n \geq 5$ embryos/group) (C). (D–G) Comparison of the number of Pax7$^+$ myoblasts in the EDL muscle at E15.5. (D, E) Representative images of Pax7 immunofluorescence (red). Green, myofibers (autofluorescence). No difference was observed in the percentage of Pax7$^+$ cells in the EDL (F); however, *Smyd1* CKO muscle exhibited less myofibers per Pax7$^+$ cell (G) ($n \geq 6$ embryos/group). (H–J) Comparison of the number of fibers relative to myoblasts in the EDL muscle at E15.5. Myoblasts were identified as non-myofiber YFP$^+$ cells. YFP expression is the result of recombination of the *Rosa26*^{YFP} allele by *Myf5*^{cre} and represents the *Myf5* lineage. (H, I) Representative images of immunofluorescence for YFP (green) and MyHC (red). (J) *Smyd1* CKO muscle exhibited less myofibers per myoblast ($n \geq 5$ embryos/group). (K–M) Comparison of myoblast proliferation within the EDL at E15.5. BrdU was administered 4 h prior to sacrifice. (K, L) Representative images of YFP (green) and BrdU (red) immunofluorescence. No difference was observed in the percentage of BrdU$^+$ myoblasts (double positive cells) (M) ($n \geq 5$ embryos/group). (N, O) Comparison of apoptosis within the EDL at E15.5 by TUNEL assay (red). No difference was observed ($n \geq 5$ embryos/group). (P–R) Comparison of the number of Myog$^+$ cells in the EDL at E16.5. (P, Q) Representative images of Myog immunofluorescence (red). *Smyd1* CKO exhibited a higher percentage of Myog$^+$ cells than controls (R) ($n=6$ embryos/group). Blue, nuclei (DAPI). Scale bars are 50 μm (A, B, D, E, N, O) and 20 μm (H, I, K, L, P, Q). $^*P < 0.05$, $^{**}P < 0.01$, Student's *t* test. Error bars indicate SEM. Ctrl, control; CKO, conditional knockout; YFP, yellow fluorescent protein; MyHC, myosin heavy chain; BrdU, bromodeoxyuridine; TUNEL, terminal deoxynucleotidyl transferase dUTP nick end labeling.

Sims et al., 2002). Zebrafish expressing Myc-Smyd1 show primarily cytosolic localization in both myoblasts and myotubes (Li et al., 2011). For C2C12 cells, we found Smyd1 to be both nuclear and cytoplasmic in myoblasts, but primarily cytoplasmic in myotubes. Importantly, we found that *in vivo*, as with C2C12 cells, Smyd1 protein localized to both the nucleus and cytoplasm of Myog$^+$ myoblasts within the myotome. Little to no Smyd1 was detectable in Pax7$^+$ myogenic progenitor cells and Myog$^+$ cells could be found with or without Smyd1 expression. These observations indicate that Smyd1 is downstream of Myog, becoming expressed in differentiating myoblasts. Importantly, this is the myogenic stage affected by the absence of Smyd1. *Smyd1* CKO embryos exhibited increased Myog$^+$ myoblasts and fewer myofibers. In differentiated muscle fibers, Smyd1 primarily localized to the sarcoplasm. Within the sarcoplasm, Smyd1 localized within bands opposite/non-overlapping to that of α-actinin, consistent with previous reports of Smyd1's localization to the sarcomeric M-line in zebrafish fast-twitch muscles (Just et al., 2011; Li et al., 2011).

Not only does Smyd1's subcellular localization change during myoblast differentiation, but protein levels also greatly increase and most (if not all) of the extra protein ends up in the sarcoplasm. The large increase in Smyd1 protein expression during differentiation is most apparent in western blots, where levels are almost undetectable in undifferentiated C2C12 myoblasts and extremely abundant after a few days in differentiation medium (Fig. 6A). This is also supported by immunofluorescence experiments because exposure times to detect Smyd1 in myotubes/fibers are much shorter than for myoblasts (Fig. 1P vs. F and K). Furthermore, when differentiated C2C12 cells are stained for Smyd1, the undifferentiated myoblasts in the culture appear negative because of the high abundance in the myotubes (Fig. 1D). Nuclear Smyd1 is barely detectable in myotubes/fibers *in vivo* or *in vitro*; however there appears to be low nuclear levels that are difficult to detect due to the high abundance in the sarcoplasm. Collectively, these observations support the idea that Smyd1 is both an epigenetic modulator of transcription as well as a sarcoplasmic regulator of myofibrillogenesis.

3.2. Defective second wave myogenesis

No gross abnormalities, changes in gene expression or abundance of Pax7$^+$ myoblasts were detected in *Smyd1* CKO embryos at E11.5 (Fig. 2 and Fig. 5A–C) Hence, *Smyd1* deletion did not

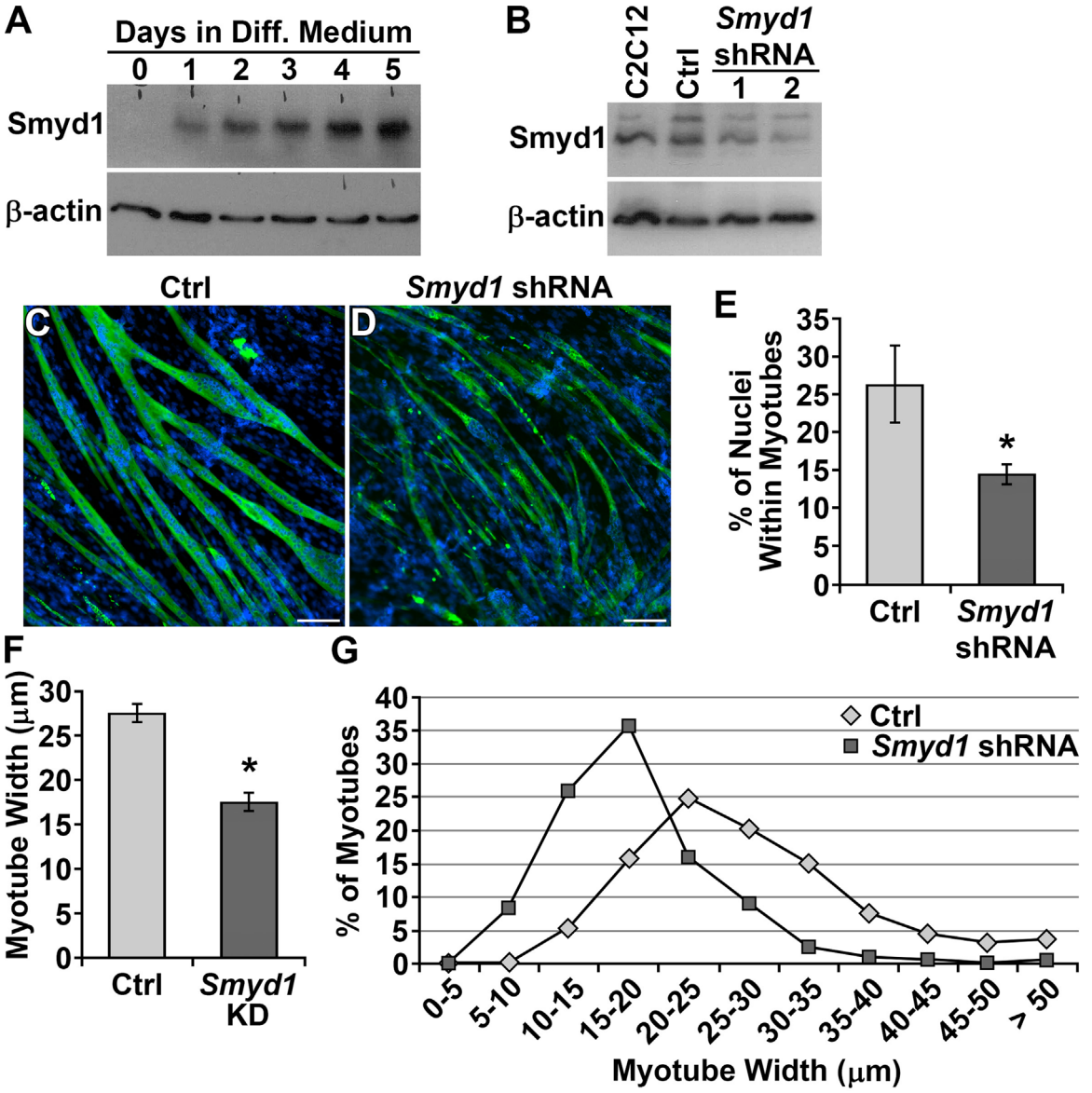

Fig. 6. *Smyd1* knockdown in C2C12 myoblasts impairs fusion and blocks myotube hypertrophy. (A, B) Western blots. Smyd1 protein expression increased throughout the course of myoblast differentiation (A). Smyd1 protein levels were reduced in cell lines stably expressing shRNA against *Smyd1* (B). The C2C12 lane contains extract from the parental cell line. The Ctrl lane contains extract from a cell line stably expressing non-specific control shRNA. (C, D) Knockdown of *Smyd1* led to thinner myotubes. Representative images of C2C12 cells expressing control shRNA (C) or *Smyd1* shRNA (D) after 5 days in differentiation medium. Myotubes were identified by immunofluorescence for myosin heavy chain (green). Blue, nuclei (DAPI). (E) *Smyd1* knockdown impaired myoblast fusion. Myoblast fusion index was calculated by dividing the number of nuclei within myotubes by the total number of nuclei ($n=9$ replicates/group). (F, G) *Smyd1* knockdown impaired myotube hypertrophy. Mean myotube width (F) and distribution of myotube widths (G) ($n=18$ replicates/group). $^{*}P<0.05$, Student's t test. Error bars indicate SEM. Scale bars are 100 μm. Ctrl, control; CKO, conditional knockout; Diff., differentiation; KD, knockdown.

appear to affect the first wave of myogenesis, which occurs from E10.5 to E12.5 in mice (Biressi et al., 2007b). However, we found reduced numbers of myofibers as well as altered gene expression for a number of skeletal muscle specific genes during the second myogenic wave, which occurs from E14.5 to E17.5 (Biressi et al., 2007b). *Smyd1* CKO embryos exhibited a greater loss of secondary than primary myofibers during the second myogenic wave. This may be due to unique functions for Smyd1 in fast-twitch fibers. Based on contractile protein expression, previous literature suggests that primary myofibers are similar to adult slow-twitch fibers and secondary fibers are more akin to adult fast-twitch fibers (Biressi et al., 2007b). *Smyd1* mutant zebrafish exhibit defective myofibrillogenesis specifically in fast-twitch fibers (Just et al., 2011). Likewise, CKO of *Smyd1* in differentiated myofibers (perinatal CKO post-myogenesis) results in centronuclear myopathy specifically in fast-twitch muscles (Stewart et al., 2016 (manuscript in review)). Our observation that loss of *Smyd1* more greatly disrupted formation of secondary fibers supports the idea that *Smyd1* may be more important for the stability and/or function of fast-twitch fibers. These data suggest that although *Smyd1* is expressed in all fiber types in mammals, it may perform selective functions in different fiber types. Smyd1's fast-twitch fiber-specific functions may be more critical for the growth and survival of myofibers during myogenesis.

We also noticed partial penetrance of the phenotype in *Smyd1* CKO embryos in terms of reduction in primary and secondary muscle fibers during the second myogenic wave. A few CKOs had a very severe loss of muscle fibers; most CKOs had a modest but

noticeable reduction. Such variability might be due to slight differences in the timing of *Smyd1* deletion or variability in the percentage of myoblasts harboring a total loss of *Smyd1*. The mice used for this study were of a mixed B6;129 genetic background, which could conceivably contribute to this variability.

Our evidence suggests Smyd1 is important for late-stage myoblast differentiation. Both control and *Smyd1* CKO muscles exhibited similar abundance of $Pax7^+$ myogenic progenitor cells, rates of proliferation and apoptosis in the EDL at E15.5, the midpoint of the second myogenic wave. We found no evidence for degeneration as *Smyd1* CKOs did not exhibit TUNEL positive myofibers, alterations in atrophy gene expression or reduction in myofiber diameter. What we did find was fewer myofibers relative to myoblasts and increased numbers of $Myog^+$ myoblasts. These data suggest impaired myoblast differentiation and are consistent with the impaired myoblast fusion observed for *Smyd1* knockdown C2C12 cells.

The stage in mouse embryogenesis when motor neurons first make contact with developing muscle fibers is also during the second myogenic wave (Rossi and Messina, 2014). Interaction between newly forming muscle fibers and neurons is necessary for further development of myofibers. Failure of motor neurons to properly interact with developing myofibers leads to dis-integration of both primary and secondary muscle fibers, with the latter being more severely affected (Biressi et al., 2007a). This phenotype is very similar to what we observe in our *Smyd1* CKO mouse embryos. Hence it is possible that Smyd1 plays a role in relaying a survival cue from newly formed neuromuscular junctions. However, data from C2C12 cells argues against this being the primary defect. Knock-down of *Smyd1* expression in C2C12 cells led to hypotrophic, poorly differentiated myotubes with reduced fusion index and impaired myofiber growth. These *in vitro* data do not support the idea that myofiber loss was due to negative effects on innervation, but rather due to intrinsic effects on myoblast differentiation or myofiber growth. It appears from immunofluorescence experiments that individual *Smyd1* CKO myofibers contain less total MyHC protein (CKO myofibers exhibit weaker anti-MyHC fluorescence intensity than control myofibers) (Fig. 4A–D and Supplementary Fig. S1). This observation implicates Smyd1 as a positive regulator of muscle gene expression underlying myofiber growth.

Smyd1 CKO embryos showed altered expression of three major myogenic transcription factors (*Pax3*, *Myf5* and *Myf6*) only during the second wave of myogenesis (Fig. 4G, I, K). Reduced *Myf5* expression, which is temporally downstream of *Pax7* during myogenesis, indicates that there may be a defect in myoblast differentiation or that Smyd1 regulates the myoblast differentiation gene expression program. Reduced expression of *Myf5* was not the result of the $Myf5^{cre}$ knock-in because our control embryos also expressed *cre* (Controls were $Myf5^{cre/+}$; $Smyd1^{flox/+}$). Increased expression of *Pax3* could be due to a compensatory feedback loop due to impaired myoblast differentiation. *Pax3* is more highly expressed in primary wave myoblasts and myofibers than in their secondary wave counterparts (Biressi et al., 2007b). Thus, increased *Pax3* expression opens the possibility that *Smyd1* CKO fetal myoblasts retain the gene expression signature of embryonic myoblasts, which may impair second wave myogenesis. Alternatively, increased *Pax3* could simply reflect the increased ratio of primary to secondary myofibers. *Myf6* is expressed late during myogenesis and it is the only MRF expressed in mature myofibers (Rhodes and Konieczny, 1989). Reduced *Myf6* expression would impair myofiber development, as seen in the *Smyd1* CKO; however, decreased *Myf6* mRNA could be a consequence of less total myofibers.

In zebrafish embryos, *Smyd1* knockdown did not affect the mRNA levels of slow and fast myosin isoforms, but did affect their protein levels (Li et al., 2013). It was apparent from anti-MyHC immunofluorescence that *Smyd1* CKO myofibers have less total MyHC protein than controls (Fig. 4A–D and Supplementary Fig. S1). Thus, our data are consistent with those from zebrafish models, in that loss of *Smyd1* resulted in reduced MyHC protein; however, we also observed reduced gene expression for several MyHC isoforms (*Myh3*, *Myh7* and *Myh8*) and α-actin (*Acta1*) (Fig. 4M–P). These alterations in gene expression could be a consequence of fewer myofibers, but also support the idea that Smyd1 positively regulates contractile protein gene expression. The latter hypothesis is supported by a recent article indicating that Smyd1 is essential for activation of muscle genes in rhabdomyosarcoma (Coda et al., 2015).

3.3. Edema and embryonic lethality

Smyd1 CKO embryos are motionless when recovered on E17.5 or E18.5 and consistently die perinatally (Table 1). A very similar phenotype, including dorsal subcutaneous edema and perinatal lethality, was observed when *Smyd1* was deleted using *Myog-cre*, (Rasmussen and Tucker, unpublished observations). These data indicate that muscle contraction becomes impaired over time—essentially a mild version of the phenotype reported for zebrafish *Smyd1* mutants or knock-downs where muscle contraction was completely absent from myofiber inception (Just et al., 2011). Failed myofibrillogenesis in zebrafish is thought to result from improper myosin folding or assembly (Just et al., 2011).

Almost all *Smyd1* CKOs exhibited subcutaneous edema reminiscent of the "amorphous connective tissue" reported for the *Myf5*/*MyoD* double knock-out mouse (Rudnicki et al., 1993), which completely lacks skeletal muscle. Thus, subcutaneous edema could be the consequence of muscle loss. Edema could also be the consequence of impaired circulation or lymphatic drainage. This is puzzling as *Smyd1* expression is restricted to striated muscles and $CD8^+$ T lymphocytes (Gottlieb et al., 2002; Hwang and Gottlieb, 1997). $Myf5^+$ progenitors give rise to skeletal muscle, brown adipose, some rib cartilage, dorsal skin and connective tissues ((Haldar et al., 2008) and Fig. 3C, D). Thus, vessels along the dorsal aspect of the embryo could be impacted by $Myf5^{cre}$. But, even if $Myf5^{cre}$ catalyzed *Smyd1* deletion in other tissues, it is unlikely to have an effect because *Smyd1* is not expressed in those tissues. This suggests depletion of Smyd1 from the skeletal muscle lineage has a non-cell autonomous effect on the circulatory/lymphatic system. We looked for heart defects, but found no obvious morphological abnormalities by histological analysis and there was no pericardial edema (data not shown). Although the striated muscle-specific expression pattern is well-documented, *Smyd1* could be expressed in a non-muscle cell type that is also in the *Myf5* lineage and important for proper circulation (e.g. dorsal smooth muscle or endothelial cells). The other members of the SMYD family (*Smyd2 - 5*) exhibit broad expression in many cell types. Thus, it is not unreasonable to hypothesize that *Smyd1* expression is broader than currently known.

Collectively, our results indicate that inception of the skeletal myogenesis program does not require Smyd1, but downstream events do. Elimination of Smyd1 impairs myofiber development and alters myogenic gene expression during the second wave of mammalian skeletal myogenesis. In zebrafish, *Smyd1* is only critical for sarcomerogenesis in fast-twitch myofibers (Just et al., 2011). In contrast, in mice, where both fast- and slow-twitch fibers are multi-nucleated and interspersed, Smyd1 appears to be necessary for proper development of both fiber types during embryogenesis. Based on our studies and the current literature, Smyd1 is multi-functional and vital for diverse aspects of muscle biology via epigenetic effects on gene expression and protein–protein interactions that facilitate myofibrillogenesis. A

challenging future objective is to identify the promoter/enhancer regions targeted by Smyd1 histone methyltransferase action and to determine the accompanying epigenetic consequences *in vivo*.

4. Materials and methods

4.1. Animals

Smyd1$^{flox/flox}$ mice were developed in collaboration with Dr. Haley Tucker (University of Texas, Austin) (Rasmussen et al., 2015). *Smyd1*$^{+/-}$ mice were generated by crossing *Smyd1*$^{flox/flox}$ to the maternal deleter *Tg(Sox2-cre)* (Hayashi et al., 2003) (Jackson Laboratory, stock #8454). *Rosa26*$^{YFP/YFP}$ and *Myf5*$^{cre/+}$ mice were obtained from the Jackson Laboratory (stock #7903 and #10529, respectively). Mice for experimental analysis were obtained from the following cross: *Myf5*$^{cre/+}$; *Smyd1*$^{+/-}$ x *Smyd1*$^{flox/flox}$; *Rosa26*$^{YFP/YFP}$. Controls were *Myf5*$^{cre/+}$; *Smyd1*$^{flox/+}$; *Rosa26*$^{YFP/+}$. CKOs were *Myf5*$^{cre/+}$; *Smyd1*$^{flox/-}$; *Rosa26*$^{YFP/+}$.

The following primers were used for genotyping: Cre-F: 5′-GCC ACC AGC CAG CTA TCA ACT C, Cre-R: 5′-TTG CCC CTG TTT CAC TAT CCA G, Smyd1-F: 5′-TCA TGA GAT GGG CAT GAG CC, Smyd1-R1 5′-GCA TAC GCA CAT GTG CTC GC, Smyd1-R2: 5′-CTC ACT TGC GTC CCA GTA CTT G. Smyd1-F/R1 identifies wild-type and flox alleles (432 bp and 552 bp, respectively). Smyd1-F/R2 identifies the null allele (~500 bp). Mice were euthanized by CO_2 inhalation followed by cervical dislocation. All experimental procedures involving mice were approved by the Institutional Animal Care and Use Committee of the University of Houston.

4.2. Tissue collection

Embryos were manually dissected in PBS immediately after euthanasia. For RNA or protein extraction, tissues were snap frozen in liquid nitrogen and stored at −80 °C. For H&E staining, tissues were fixed by overnight immersion in Bouin's fluid. For immunofluorescence, tissues were fixed overnight in 4% PFA in PBS and rinsed in 70% ethanol for ≥25 h prior to tissue processing. All tissues were dehydrated through a standard ethanol gradient, cleared in Histoclear (National Diagnostics, cat# HS-200) and embedded in Paraplast Plus® Tissue Embedding Medium (Statlab, cat# 2004). Seven to eight micron sections were prepared for histology.

4.3. Wholemount in situ hybridization

Wholemount *in situ* hybridization was performed following a standard protocol (Nagy, 2003). Digoxigenin (DIG)-labeled complementary RNA probes were prepared using a DIG RNA Labeling Kit (Roche, cat# 11 175 025 910). Hybridization and wash steps were automated using an InsituPro robot (Intavis AG). Hybridized probes were visualized by a color reaction using alkaline phosphatase-conjugated anti-DIG Fab fragments (Roche, cat# 11 093 274 910) and nitroblue tetrazolium and bromochloroindolyl phosphate (NBT-BCIP) reagents (Roche, cat# 11 681 451 001). Embryos were post-fixed in 4% paraformaldehyde-PBS and imaged in PBS. Probe sequence information is available upon request.

4.4. Western blotting

Western blot assays were carried out with either C2C12 whole cell extracts obtained using RIPA buffer or frozen E16.5 embryos with head and internal organs removed homogenized in T-PER buffer (Life Technologies) according to the manufacturer's instructions. Lysis buffers were supplemented with protease and phosphatase inhibitors. The cell lysate was centrifuged at 10,000 x g for 5 min. 50 μg of supernatant protein was solubilized in Laemmli Buffer and separated by 4–20% SDS-PAGE (Mini Protean II System, Bio-Rad Laboratories, Hercules, CA). The proteins were transferred onto 0.2 μm nitrocellulose membranes (Bio-Rad Laboratories). Membranes were blocked with 5% non-fat milk-TBST for 1 h at room temperature. Primary antibodies recognizing Smyd1 (Santa Cruz, cat# sc-79080), MyHC (Developmental Studies Hybridoma Bank, clone MF-20) or β-actin-HRP (Santa Cruz I-19, cat# sc-1616) were diluted in 2.5% non-fat milk-TBST. Following overnight incubation at 4 °C with primary antibody, membranes were washed with TBST and then incubated with the appropriate horseradish peroxidase-conjugated secondary antibody for 3 h at room temperature. Membranes were washed again, and visualized by chemiluminescence using SuperSignal West Pico Chemiluminescent Substrate (Thermo Scientific, Rockford, IL). Mean pixel intensity of western blot band was calculated using ImageJ software v1.48 (National Institutes of Health, USA).

4.5. Histological analyses

H&E staining was performed using a standard protocol. Immunofluorescence was performed on 8 μm paraffin sections using 1x casein-PBST (Vector Labs) for blocking and 10% normal serum (Vector Labs) in PBST as the antibody diluent. Primary antibodies were incubated overnight at 4 °C. Secondary antibodies were incubated for 1 h at room temperature. All slides were counterstained with DAPI and coverslips mounted with Vecta-Shield hard set mounting medium (Vector Labs). Primary antibodies used were as follows: Smyd1 (Santa Cruz, cat# sc-79080), MyHC (Developmental Studies Hybridoma Bank, clone MF-20), α-actinin (clone EA-53, Sigma-Aldrich, cat# A7811), GFP (Abcam, cat# ab6662) and Pax7 (Developmental Studies Hybridoma Bank).

To assay cell proliferation, pregnant mice were weighed and injected with 10 ml/kg BrdU Labeling Reagent (Invitrogen, catalog# 00-0103) 4 h before sacrifice. Immunofluorescence was performed as described above with anti-BrdU monoclonal antibodies (Developmental Studies Hybridoma Bank, clone G3G4). Apoptosis was assayed using the Click-iT ® Plus TUNEL Assay kit (Life technologies, Catalog#C10618) according to the manufacturer's instructions.

4.6. Microscopy

Stereoimages (brightfield and fluorescence) were captured with a Leica MZ10F stereomicroscope and the extended depth of focus feature of LAS v3.7 software (Leica Microsystems, Wetzlar, Germany). Brightfield and epifluorescence images of tissues sections were obtained using a Nikon Ti-E inverted microscope equipped with a DS-Fi1 5-megapixel color camera (Nikon Instruments), a CoolSNAP HQ2 14-bit monochrome camera (Photometrics, Tucson, AZ) and NIS Elements software v4.13 (Nikon Instruments).

4.7. Real-time PCR

Total RNA was extracted from whole E11.5 embryos or E15.5 embryos with head and internal organs removed using TRIzol reagent according to the manufacturer's protocol (Life Technologies, Carlsbad, CA). mRNA levels were measured using TaqMan gene expression assays with 6-carboxyfluorescein (FAM)-labeled probes from Applied Biosystems (Life Technologies) (Mm01332463_m1 for *Myh3*, Mm01319006_g1 for *Myh7*, Mm01329494_m1 for *Myh8*, Mm01203489_g1 for *Myod1*, Mm01354484_m1 for *Pax7*, Mm00468267_m1 for *Eno3*, Mm01321487_m1 for *Ckm*,Mm00808218_g1 for *Acta1*, Mm01185221_m1 for *Trim63*, Mm00499523_m1 for *Fbxo32*) and

custom oligos for *Pax3* (Pax3-F: 5′-CCA GAG GGC GAA GCT TAC C, Pax3-R: 5′-GTT GAT TGG CTC CAG CTT GTT T, Pax3-Probe: 5′-TCT GGT TTA GCA ACC GCC GTG CA), *Myf5* (Myf5-F: 5′- AGC AGC TTT GAC AGC ATC TAC TGT, Myf5-R: 5′-AAT GCT GGA CAA GCA ATC CAA, Myf5-Probe: 5′-TGC TGC AGA TAA AAG CTC CGT GTC CA) and *Myf6* (Myf6-F: 5′- AGC TAC AAA CCC AAG CAA GAA ATT, Myf6-R: 5′-CCT GGA ATG ATC CGA AAC ACT T, Myf6-Probe: 5′-TGC GGA TTT CCT GCG CAC CTG) (Biosearch Technologies, Petaluma, CA). The level of *Gapdh* mRNA was used for normalization. The PCR was run using an ABI Prism 7900HT thermocycler and SDS2.1 software (Applied Biosystems). Data were analyzed by the comparative ΔΔCT method.

4.8. Cell culture

The mouse skeletal myoblast cell line C2C12 was obtained from ATCC (cat# CRL-1772). C2C12 cells were routinely cultured in their undifferentiated state in high glucose DMEM supplemented with 20% fetal bovine serum and 1X antibiotic–antimycotic (Life Technologies, cat# 15240-096) at 37 °C and 5% CO_2. Differentiation was induced by switching the medium to high glucose DMEM supplemented with 2% horse serum and 1 μg/ml insulin after the cells reached about 90% confluence. Differentiating C2C12 cells were supplied with fresh differentiation medium every 24 h and maintained at 37 °C and 5% CO_2.

Control and *Smyd1* knockdown C2C12 cell lines were generated using GIPZ lentiviral particles encoding short hairpin-RNA against *Smyd1* (Thermo-scientific, source clone ID# V3LMM_480880, V2LMM_61704, V3LMM_480879) and non-silencing control *sh*RNA (catalog # RHS4348) according to the manufacturer's instructions. Successfully transduced cells were selected by puromycin treatment.

4.9. Statistical analyses

For studies with two experimental groups, an independent samples Student's *t*-test was performed. Prior to *t*-test, an *F*-test was performed to determine if the variances of the two groups were equal. If $P < 0.05$ for the *F*-test (unequal variances), the test was repeated with log-transformed data. If log-transformed data showed unequal variances, the *t*-test was performed with a correction for unequal variances (Welch test). Embryonic lethality data (expected vs. observed genotypes) were analyzed by the Fisher's exact test. A *P*-value of < 0.05 was considered significant for all tests.

Acknowledgments

The BrdU (G3G4), MyHC (MF-20) and Pax7 and monoclonal antibodies used in this study were obtained from the Developmental Studies Hybridoma Bank, created by the NICHD of the NIH and maintained at The University of Iowa, Department of Biology, Iowa City, IA. This work was supported by the American Heart Association [12BGIA11860006 to M.D.S.]; the University of Houston Division of Research Small Grants Program [1HOU08 to M.D.S.]; and the Texas Heart Institute [M.D.S. and R.J.S.].

Appendix A. Supplementary material

Supplementary data associated with this article can be found in the online version at http://dx.doi.org/10.1016/j.ydbio.2015.12.005.

References

Berkholz, J., Michalick, L., Munz, B., 2014. The E3 SUMO ligase Nse2 regulates sumoylation and nuclear-to-cytoplasmic translocation of skNAC-Smyd1 in myogenesis. J. Cell Sci. 127, 3794–3804.
Biressi, S., Molinaro, M., Cossu, G., 2007a. Cellular heterogeneity during vertebrate skeletal muscle development. Dev. Biol. 308, 281–293.
Biressi, S., Tagliafico, E., Lamorte, G., Monteverde, S., Tenedini, E., Roncaglia, E., Ferrari, S., Ferrari, S., Cusella-De Angelis, M.G., Tajbakhsh, S., Cossu, G., 2007b. Intrinsic phenotypic diversity of embryonic and fetal myoblasts is revealed by genome-wide gene expression analysis on purified cells. Dev. Biol. 304, 633–651.
Cho, H.S., Hayami, S., Toyokawa, G., Maejima, K., Yamane, Y., Suzuki, T., Dohmae, N., Kogure, M., Kang, D., Neal, D.E., Ponder, B.A., Yamaue, H., Nakamura, Y., Hamamoto, R., 2012. RB1 methylation by SMYD2 enhances cell cycle progression through an increase of RB1 phosphorylation. Neoplasia 14, 476–486.
Coda, D.M., Lingua, M.F., Morena, D., Foglizzo, V., Bersani, F., Ala, U., Ponzetto, C., Taulli, R., 2015. SMYD1 and G6PD modulation are critical events for miR-206-mediated differentiation of rhabdomyosarcoma. Cell Cycle 14, 1389–1402.
Du, S.J., Rotllant, J., Tan, X., 2006. Muscle-specific expression of the smyd1 gene is controlled by its 5.3-kb promoter and 5'-flanking sequence in zebrafish embryos. Dev. Dyn. 235, 3306–3315.
Gao, J., Li, J., Li, B.J., Yagil, E., Zhang, J., Du, S.J., 2014. Expression and functional characterization of Smyd1a in myofibril organization of skeletal muscles. PLoS One 9, e86808.
Gottlieb, P.D., Pierce, S.A., Sims, R.J., Yamagishi, H., Weihe, E.K., Harriss, J.V., Maika, S. D., Kuziel, W.A., King, H.L., Olson, E.N., Nakagawa, O., Srivastava, D., 2002. Bop encodes a muscle-restricted protein containing MYND and SET domains and is essential for cardiac differentiation and morphogenesis. Nat. Genet. 31, 25–32.
Haldar, M., Hancock, J.D., Coffin, C.M., Lessnick, S.L., Capecchi, M.R., 2007. A conditional mouse model of synovial sarcoma: insights into a myogenic origin. Cancer Cell 11, 375–388.
Haldar, M., Karan, G., Tvrdik, P., Capecchi, M.R., 2008. Two cell lineages, myf5 and myf5-independent, participate in mouse skeletal myogenesis. Dev. Cell. 14, 437–445.
Hayashi, S., Tenzen, T., McMahon, A.P., 2003. Maternal inheritance of Cre activity in a Sox2Cre deleter strain. Genesis 37, 51–53.
Huang, J., Perez-Burgos, L., Placek, B.J., Sengupta, R., Richter, M., Dorsey, J.A., Kubicek, S., Opravil, S., Jenuwein, T., Berger, S.L., 2006. Repression of p53 activity by Smyd2-mediated methylation. Nature 444, 629–632.
Hwang, I., Gottlieb, P.D., 1997. The Bop gene adjacent to the mouse CD8b gene encodes distinct zinc-finger proteins expressed in CTLs and in muscle. J. Immunol. 158, 1165–1174.
Just, S., Meder, B., Berger, I.M., Etard, C., Trano, N., Patzel, E., Hassel, D., Marquart, S., Dahme, T., Vogel, B., Fishman, M.C., Katus, H.A., Strahle, U., Rottbauer, W., 2011. The myosin-interacting protein SMYD1 is essential for sarcomere organization. J. Cell Sci. 124, 3127–3136.
Kawamura, S., Yoshigai, E., Kuhara, S., Tashiro, K., 2008. smyd1 and smyd2 are expressed in muscle tissue in Xenopus laevis. Cytotechnology 57, 161–168.
Li, D., Niu, Z., Yu, W., Qian, Y., Wang, Q., Li, Q., Yi, Z., Luo, J., Wu, X., Wang, Y., Schwartz, R.J., Liu, M., 2009. SMYD1, the myogenic activator, is a direct target of serum response factor and myogenin. Nucleic Acids Res. 37, 7059–7071.
Li, H., Xu, J., Bian, Y.H., Rotllant, P., Shen, T., Chu, W., Zhang, J., Schneider, M., Du, S.J., 2011. Smyd1b_tv1, a key regulator of sarcomere assembly, is localized on the M-line of skeletal muscle fibers. PLoS One 6, e28524.
Li, H., Zhong, Y., Wang, Z., Gao, J., Xu, J., Chu, W., Zhang, J., Fang, S., Du, S.J., 2013. Smyd1b is required for skeletal and cardiac muscle function in zebrafish. Mol. Biol. Cell. 24, 3511–3521.
Luo, X.G., Zhang, C.L., Zhao, W.W., Liu, Z.P., Liu, L., Mu, A., Guo, S., Wang, N., Zhou, H., Zhang, T.C., 2014. Histone methyltransferase SMYD3 promotes MRTF-A-mediated transactivation of MYL9 and migration of MCF-7 breast cancer cells. Cancer Lett. 344, 129–137.
Mazur, P.K., Reynoird, N., Khatri, P., Jansen, P.W., Wilkinson, A.W., Liu, S., Barbash, O., Van Aller, G.S., Huddleston, M., Dhanak, D., Tummino, P.J., Kruger, R.G., Garcia, B.A., Butte, A.J., Vermeulen, M., Sage, J., Gozani, O., 2014. SMYD3 links lysine methylation of MAP3K2 to Ras-driven cancer. Nature 510, 283–287.
Nagy, A., 2003. Manipulating the Mouse Embryo: A Laboratory Manual, 3rd ed. Cold Spring Harbor Laboratory Press, Cold Spring Harbor, NY.
Phan, D., Rasmussen, T.L., Nakagawa, O., McAnally, J., Gottlieb, P.D., Tucker, P.W., Richardson, J.A., Bassel-Duby, R., Olson, E.N., 2005. BOP, a regulator of right ventricular heart development, is a direct transcriptional target of MEF2C in the developing heart. Development 132, 2669–2678.
Piao, L., Kang, D., Suzuki, T., Masuda, A., Dohmae, N., Nakamura, Y., Hamamoto, R., 2014. The histone methyltransferase SMYD2 methylates PARP1 and promotes poly(ADP-ribosyl)ation activity in cancer cells. Neoplasia 16, 257–264 264 e252.
Rasmussen, T.L., Ma, Y., Park, C.Y., Harriss, J., Pierce, S.A., Dekker, J.D., Valenzuela, N., Srivastava, D., Schwartz, R.J., Stewart, M.D., Tucker, H.O., 2015. Smyd1 Facilitates Heart Development by Antagonizing Oxidative and ER Stress Responses. PLoS One 10, e0121765.
Rhodes, S.J., Konieczny, S.F., 1989. Identification of MRF4: a new member of the muscle regulatory factor gene family. Genes. Dev. 3, 2050–2061.
Rossi, G., Messina, G., 2014. Comparative myogenesis in teleosts and mammals. Cell. Mol. Life Sci. 71, 3081–3099.
Rudnicki, M.A., Schnegelsberg, P.N., Stead, R.H., Braun, T., Arnold, H.H., Jaenisch, R., 1993. MyoD or Myf-5 is required for the formation of skeletal muscle. Cell 75,

1351–1359.
Saddic, L.A., West, L.E., Aslanian, A., Yates 3rd, J.R., Rubin, S.M., Gozani, O., Sage, J., 2010. Methylation of the retinoblastoma tumor suppressor by SMYD2. J. Biol. Chem. 285, 37733–37740.
Sajjad, A., Novoyatleva, T., Vergarajauregui, S., Troidl, C., Schermuly, R.T., Tucker, H. O., Engel, F.B., 2014. Lysine methyltransferase Smyd2 suppresses p53-dependent cardiomyocyte apoptosis. Biochim. Biophys. Acta 1843, 2556–2562.
Sims 3rd, R.J., Weihe, E.K., Zhu, L., O'Malley, S., Harriss, J.V., Gottlieb, P.D., 2002. m-Bop, a repressor protein essential for cardiogenesis, interacts with skNAC, a heart- and muscle-specific transcription factor. J. Biol. Chem. 277, 26524–26529.
Stewart, M.D., Lopez, S., Nagandla, H., Soibam, B., Benham, A., Nguyen, J., Valenzuela, N., Wu, H.J., Burns, A.R., Rasmussen, T.L., Tucker, H.O., Schwartz, R.J., 2015. Skeletal muscle-specific loss of the SMYD1 methyltransferase causes centronuclear myopathy. 2016.
Spellmon, N., Holcomb, J., Trescott, L., Sirinupong, N., Yang, Z., 2015. Structure and function of SET and MYND domain-containing proteins. Int. J. Mol. Sci. 16, 1406–1428.
Tan, X., Rotllant, J., Li, H., De Deyne, P., Du, S.J., 2006. SmyD1, a histone methyltransferase, is required for myofibril organization and muscle contraction in zebrafish embryos. Proc. Natl. Acad. Sci. USA 103, 2713–2718.
Xu, G., Liu, G., Xiong, S., Liu, H., Chen, X., Zheng, B., 2015. The histone methyltransferase Smyd2 is a negative regulator of macrophage activation by suppressing interleukin 6 (IL-6) and tumor necrosis factor alpha (TNF-alpha) production. J. Biol. Chem. 290, 5414–5423.
Yang, J., Everett, A.D., 2009. Hepatoma-derived growth factor represses SET and MYND domain containing 1 gene expression through interaction with C-terminal binding protein. J. Mol. Biol. 386, 938–950.